



UNIVERSITY
OF WOLLONGONG
AUSTRALIA

University of Wollongong
Research Online

Faculty of Engineering - Papers (Archive)

Faculty of Engineering and Information Sciences

2012

Dielectric relaxation in the $\text{DyMn}_{1-x}\text{Fe}_x\text{O}_3$ system

Fang Hong

University of Wollongong, fh640@uowmail.edu.au

Zhenxiang Cheng

University of Wollongong, cheng@uow.edu.au

Shujun Zhang

Pennsylvania State University

Xiaolin Wang

University of Wollongong, xiaolin@uow.edu.au

<http://ro.uow.edu.au/engpapers/5192>

Publication Details

Hong, F., Cheng, Z., Zhang, S. & Wang, X. (2012). Dielectric relaxation in the $\text{DyMn}_{1-x}\text{Fe}_x\text{O}_3$ system. *Journal of Applied Physics*, 111 (3), 034104-1-034104-4.

Research Online is the open access institutional repository for the University of Wollongong. For further information contact the UOW Library:
research-pubs@uow.edu.au

Dielectric relaxation in the DyMn_{1-x}FexO₃ system

Fang Hong, Zhenxiang Cheng, Shujun Zhang, and Xiaolin Wang

Citation: *J. Appl. Phys.* **111**, 034104 (2012); doi: 10.1063/1.3681807

View online: <http://dx.doi.org/10.1063/1.3681807>

View Table of Contents: <http://jap.aip.org/resource/1/JAPIAU/v111/i3>

Published by the [American Institute of Physics](#).

Related Articles

Dielectric relaxation study of amorphous TiTaO thin films in a large operating temperature range
J. Appl. Phys. **112**, 094104 (2012)

Gate stack dielectric degradation of rare-earth oxides grown on high mobility Ge substrates
J. Appl. Phys. **112**, 094501 (2012)

Magnetic and electrical properties of In doped cobalt ferrite nanoparticles
J. Appl. Phys. **112**, 084321 (2012)

Solvated dissipative electro-elastic network model of hydrated proteins
JCP: BioChem. Phys. **6**, 10B620 (2012)

Solvated dissipative electro-elastic network model of hydrated proteins
J. Chem. Phys. **137**, 165101 (2012)

Additional information on *J. Appl. Phys.*

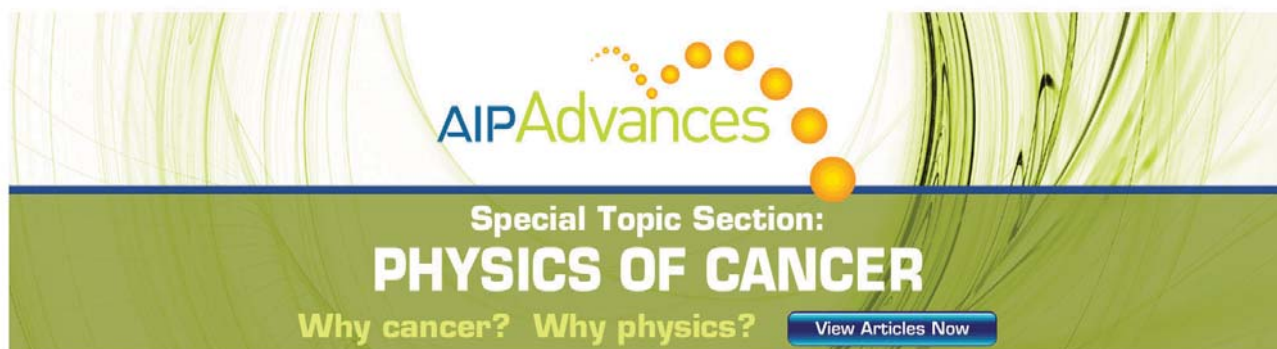
Journal Homepage: <http://jap.aip.org/>

Journal Information: http://jap.aip.org/about/about_the_journal

Top downloads: http://jap.aip.org/features/most_downloaded

Information for Authors: <http://jap.aip.org/authors>

ADVERTISEMENT



AIPAdvances

Special Topic Section:
PHYSICS OF CANCER

Why cancer? Why physics? [View Articles Now](#)

Dielectric relaxation in the $\text{DyMn}_{1-x}\text{Fe}_x\text{O}_3$ system

Fang Hong,¹ Zhenxiang Cheng,^{1,a)} Shujun Zhang,² and Xiaolin Wang¹

¹*Institute for Superconducting and Electronic Materials, University of Wollongong, Wollongong, New South Wales 2519, Australia*

²*Materials Research Institute, Pennsylvania State University, University Park, Pennsylvania 16802, USA*

(Received 22 November 2011; accepted 11 January 2012; published online 3 February 2012)

The dielectric constant and loss of perovskite $\text{DyMn}_{1-x}\text{Fe}_x\text{O}_3$ samples show strong dispersion in various frequencies, which is indicative of relaxation. The activation energies were obtained through Arrhenius law fitting and range from 0.213 eV to 0.385 eV. The Fe content dependence of the characteristic frequency f_0 and the activation energy E_α shows two transitions that are well consistent with the change in orbital ordering. Meanwhile, different magnetic orderings could affect the relaxation and induce the change in E_α . © 2012 American Institute of Physics.

[doi:10.1063/1.3681807]

I. INTRODUCTION

The giant magnetoresistance effect has aroused great interest in physics during the past several years and has been widely used in electronic memory storage.^{1,2} The next generation memory and computation devices are expected to be based on multiferroic materials, in which the spin degree of freedom can be controlled apart from the charge degree of freedom.^{3–6} A great amount of work has been done to explore mutual control of these two degrees of freedoms, the so-called magnetoelectric (ME) coupling.^{7–9} On the other hand, the dielectric property changes around the magnetic phase transition can offer a way to achieve magnetodielectric coupling,^{10–13} which also provides an alternative way to achieve more operation of degrees of freedoms. Magnetic field induced dielectric constant changes are observed in metastable orthorhombic HoMnO_3 and YMnO_3 below their incommensurate antiferromagnetic (AFM) transition temperature of 42 K.¹⁴ To achieve real applications based on spin related dielectric properties, it seems to be necessary to study their frequency and temperature dependence. Recently, dielectric relaxation was studied in $\text{La}_2\text{MgMnO}_6$ (Ref. 15) and $\text{La}_2\text{NiMnO}_6$ (Refs. 16 and 17) with double perovskite structure. However, up to now, there have been few systematic studies on dielectric relaxation in a magnetic system, and there are few reports on the relation between dielectric relaxation and subtle structural change and magnetic ordering. In the multiferroic $\text{DyMn}_{1-x}\text{Fe}_x\text{O}_3$ system, there is continuous structural and magnetic evolution.¹⁸ The static Jahn-Teller orbital ordering becomes unstable and is replaced by dynamic orbital ordering as x increases from 0 to 0.5, while the collinear AFM transition temperature shifts to higher temperature. Orbital ordering disappears in the samples with $x > 0.5$, and the samples show canted AFM ordering and experience spin reorientation from canted AFM to collinear AFM at relatively low temperature. Hence, this is a good magnetic system for spin and structure related dielectric study. In this article, we report the dielectric relaxation in the

$\text{DyMn}_{1-x}\text{Fe}_x\text{O}_3$ system at low temperature over a wide frequency range. There are two transitions of x dependent activation energies, which are found to be consistent with the transitions of orbital ordering, and magnetic ordering as well. This indicates that there are probably strong correlations between dielectric relaxation, and structural and magnetic properties.

II. EXPERIMENTAL DETAILS

Polycrystalline samples of $\text{DyMn}_{1-x}\text{Fe}_x\text{O}_3$ ($x = 0, 0.1, 0.2, 0.33, 0.5, 0.6, 0.67, 0.9$) were made by the traditional solid state reaction method from Dy_2O_3 (99.9%), MnCO_3 (99.9%), and Fe_2O_3 (99.9%) powder bought from Sigma-Aldrich. Stoichiometric amounts of raw oxide powder were weighed carefully and mixed in an agate mortar, followed by pressing into pellets 15 mm in diameter at 20 MPa. Samples were calcined at 950 °C for 10 h and sintered at 1440 °C for 6 h. The crystal structures of the samples were examined by x-ray diffraction (XRD, Model: GBC MMA), using $\text{Cu K}\alpha$ radiation at $\lambda = 1.54056 \text{ \AA}$. The Rietveld refinement calculations were conducted via FULLPROF software. An Agilent 4294 A precise impedance analyzer was employed for dielectric property measurements, scanning from 1 kHz to 1 MHz.

III. RESULTS AND DISCUSSION

A. Structure

The results of structural characterization of all samples by XRD are given in Fig. 1(a). We employed Rietveld analysis to refine the diffraction patterns. All XRD patterns can be assigned to the single phase orthorhombic structure with space group $Pbnm$, and no detectable impurity phase is present. The lattice parameter dependence on the Fe content, derived from the Rietveld refinement, is shown in Fig. 1(b). With increasing Fe content, the b -axis parameter of the unit cell becomes monotonically shorter, the c -axis parameter becomes longer in a linear way, and the a -axis parameter only increases slightly. Consistent with our previous work,¹⁸ the relation $b > a > c/\sqrt{2}$ is found in samples with $x < 0.33$, showing a static Jahn-Teller (JT) distortion (cooperative

^{a)} Author to whom correspondence should be addressed. Electronic mail: cheng@uow.edu.au.

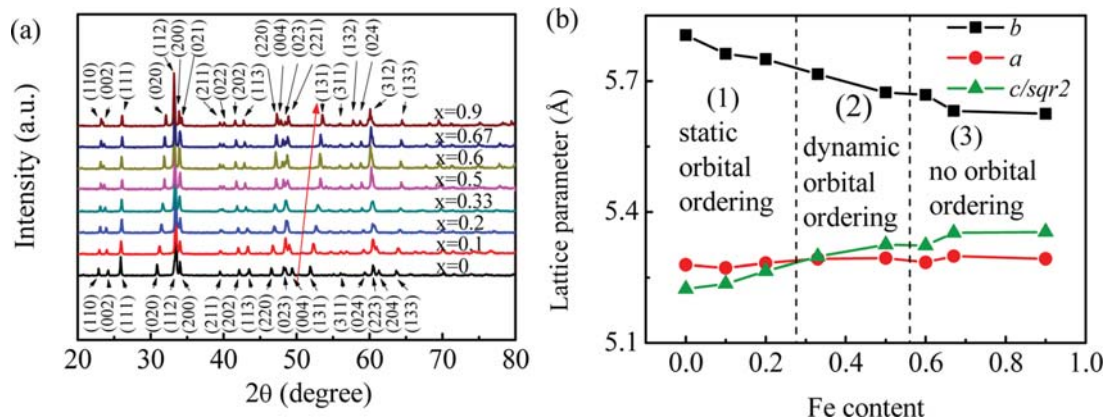


FIG. 1. (Color online) (a) X-ray diffraction patterns of all samples, (b) x dependence of lattice parameters.

antiferroic JT orbital ordering) superimposed on high temperature O-type (i.e., not JT distorted) orthorhombic structure.^{19,20} As $x > 0.33$, $a > c/\sqrt{2}$ is found. According to the reported work, the static orbital ordering is expected to be absent and replaced by weaker and weaker dynamic orbital ordering when x varies from 0.33 to 0.5, and the orbital ordering probably disappears in samples with $x > 0.5$.

B. Dielectric relaxation

The temperature dependence of the dielectric constant and loss at different frequencies is shown in Fig. 2 for representative samples with $x = 0.2$ (shown in Fig. 2(a) and 2(c)) and 0.9 (shown in Figs. 2(b) and 2(d)). Strong relaxation of the dielectric constant and loss is observed in the investi-

gated frequency range, where the temperatures of dielectric constant/loss peaks shift to higher temperature with increasing frequency. Comparing the relaxation processes between $x = 0.2$ and $x = 0.9$, it is clear that loss peak at a certain frequency also shifts strongly. This indicates that Fe doping can introduce significant change into the relaxation processes.

To calculate the activation energy of the relaxation process, we employ the modified Debye relaxation model, as shown in Eq. (1), to fit the experimental data for the sample with $x = 0$. This is because the loss peak information is difficult to extract from the loss-frequency curves.

$$\varepsilon_r = \varepsilon' + i\varepsilon'' = \varepsilon_\infty + \frac{\varepsilon_0 - \varepsilon_\infty}{1 + (i\omega\tau)^{1-\alpha}}, \quad (1)$$

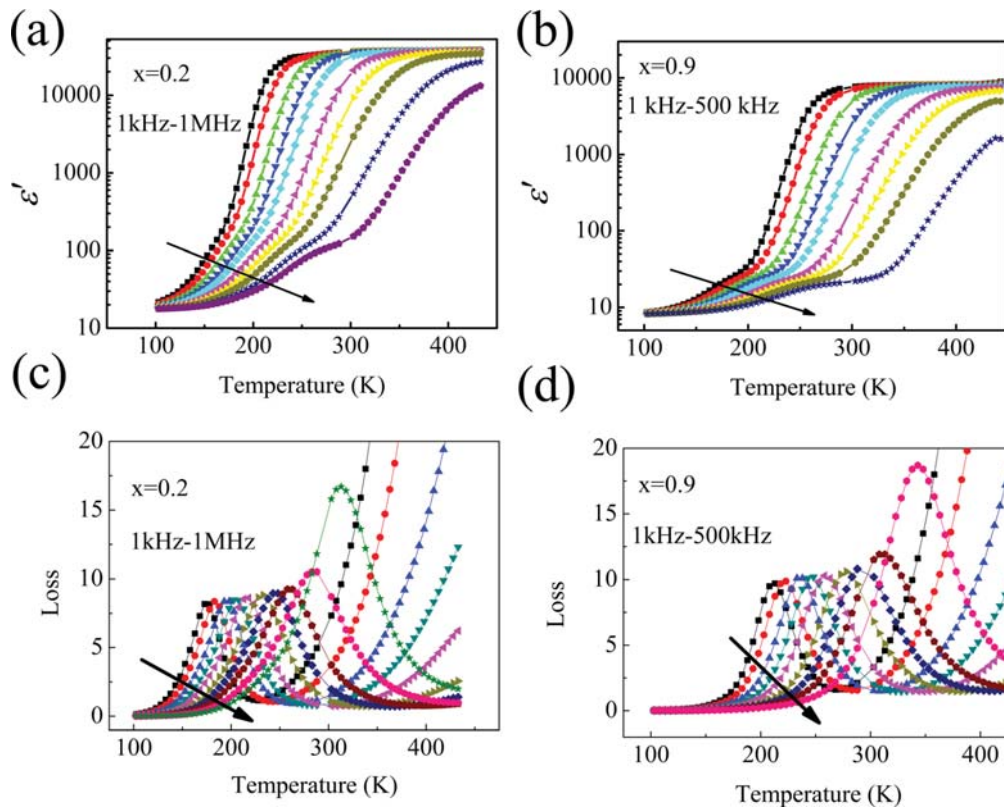


FIG. 2. (Color online) Temperature dependence of the real dielectric constants and loss for representative samples.

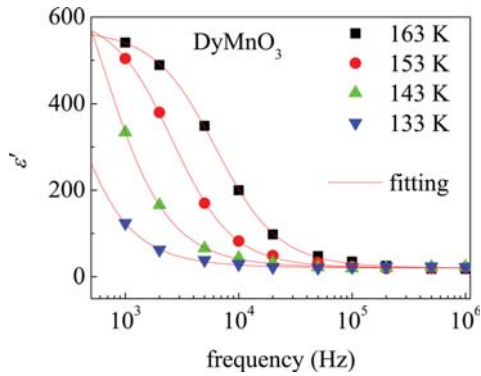


FIG. 3. (Color online) Frequency dependence of the real dielectric constant ϵ' at various temperatures: scattered symbols, experimental data; lines, the output of fitting via the modified Debye equation.

where $\epsilon_0/\epsilon_\infty$ is the static/very high frequency permittivity, ω is the angular frequency, τ is the relaxation time, and α is a parameter to describe the degree of difference from standard Debye relaxation. The data were only collected below the temperature of the loss peak in 1 kHz. The fitting results are shown in Fig. 3. A series of relaxation times τ were obtained, and it is found that they follow the Arrhenius law

$$\tau = \tau_0 \exp\left(\frac{E_x}{k_B T}\right), \quad (2)$$

where τ_0 is the relaxation time at infinite temperature (pre-exponential factor), E_x is the relaxation activation energy, k_B is the Boltzmann constant, and T is the temperature. The Arrhenius law fitting results are given in Fig. 4(a) with $E_x = 0.213$ eV and $\tau_0 = 6.43 \times 10^{-12}$ s. Considering the relaxation $\tau_0 \times f_0 = 1$, where f_0 is the characteristic frequency at infinite temperature, we can obtain an f_0 of 1.55×10^{11} Hz for the sample with $x = 0$.

For all the other samples, the dielectric loss peak can be well identified. The frequencies and temperatures of loss peaks follow the Arrhenius law

$$f = f_0 \exp\left(\frac{-E_x}{k_B T}\right), \quad (3)$$

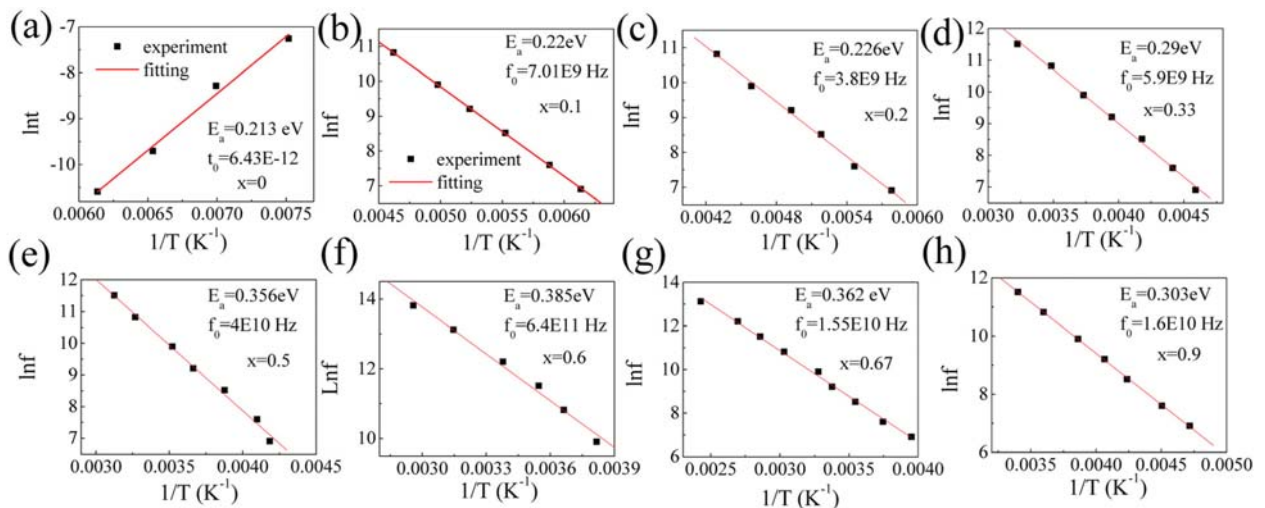


FIG. 4. (Color online) Arrhenius law fitting for all samples and corresponding activation energies at low temperature.

while the Arrhenius law fitting results are given in Figs. 4(b)–4(h).

The Fe content dependence of the characteristic frequency f_0 and activation energy E_x is shown in Fig. 5. The characteristic frequency f_0 decreases sharply from 1.55×10^{11} Hz for $x = 0$ to 3.8×10^9 Hz for $x = 0.2$, increases dramatically from $x = 0.33$ to $x = 0.6$, and then drop rapidly again when x further increases. The activation energy E_x increases slowly when x varies from 0 to 0.2 and then goes up significantly until $x = 0.6$, after which it declines quickly. Therefore, two obvious transitions of f_0 and E_x that are dependent on Fe content can be identified clearly, and they are well matched to each other.

IV. DISCUSSION

It is interesting that these two transitions correspond to structural and magnetic transitions in this system.¹⁸ The first transition between $x = 0.2$ and $x = 0.33$ is consistent with the structural change where static orbital ordering disappears and is replaced by weaker dynamic orbital ordering due to weaker Jahn-Teller distortion. The transition between $x = 0.5$ and $x = 0.6$ is found to correspond to the disappearance of dynamic orbital ordering and the appearance of spin reorientation. These two transitions are also consistent with the result reported by Chiang²¹ *et al.* In their work, the static orbital ordering becomes unstable in the sample with x around 0.3 shown in Fig. 1(b) and begins to disappear in the sample with x around 0.5 shown in Fig. 4(a) in Ref. 21. Therefore, the structural variation is probably responsible for the variation in the characteristic frequency f_0 and the activation energy E_x . Otherwise, the magnetic orderings seem to affect the relaxation as well. With x increasing from 0, the E_x increases until $x = 0.6$, during which the AFM transition temperature increases from 39 K to 400 K.¹⁸ The enhanced superexchange interaction restricts the electron transfer and consequently introduces higher E_x . For $x \geq 0.6$, spin reorientation (SR, from the canted AFM state to the collinear AFM state in this system) appears, and the transition temperature of SR decreases with increasing x .¹⁸ The relaxation process becomes easier because the canted AFM states allow a

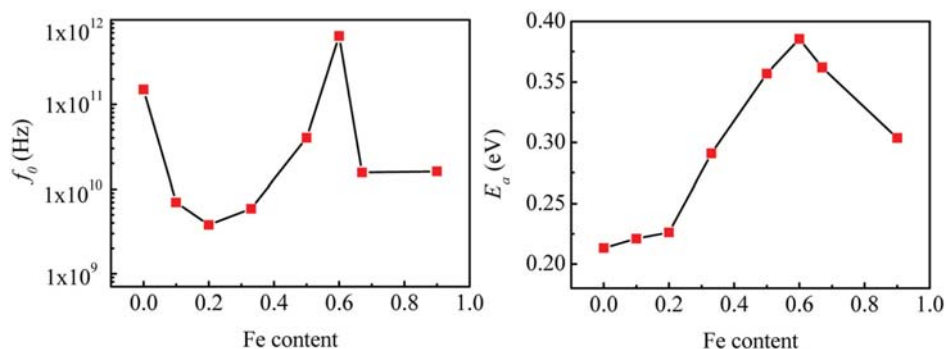


FIG. 5. (Color online) Fe content dependence of characteristic frequency f_0 (left) and activation energy E_a (right).

higher chance for electron transfer, compared with the collinear AFM state, and this effect introduces a smaller E_a . The small amounts of Mn^{4+}/Mn^{2+} and Fe^{2+} , due to the inevitable presence of oxygen defects, which occur often in manganites²² and ferrites,²³ are likely to be responsible for the relaxation process. The electron can hop in an external ac electric field between mixed-valence ions. Due to the different ionic radii of the ions with different valences, the hopping consequently induces lattice deformation and introduces polaronic distortion.

V. SUMMARY

In conclusion, we prepared perovskite $DyMn_{1-x}Fe_xO_3$ samples by solid state reaction. All samples are pure phase and show orthorhombic structure. Strong Jahn-Teller distortion is expected to favor orbital ordering in the samples with $x = 0-0.2$. However, orbital ordering becomes weaker with increasing x and disappears in the samples with $x > 0.5$. The dielectric constant and loss show strong dielectric dispersion in various frequencies, which is indicative of the relaxation. The frequencies and temperatures of the loss peaks follow the Arrhenius law, and the activation energies have been obtained, ranging from 0.23 eV to 0.36 eV. The Fe content dependence of the characteristic frequencies and activation energies shows a similar trend, which is well consistent with the change in the orbital ordering. In the light of this, dielectric and magnetic properties may be modified simultaneously by the variation in the structure because the magnetic properties of this system are also strongly related with the structure.

ACKNOWLEDGMENTS

Z.C. thanks the Australian Research Council for support through a Future Fellowship (FT 0990287).

¹Y. Moritomo, A. Asamitsu, H. Kuwahara, and Y. Tokura, *Nature* **380**, 141 (1996).

²M. B. Salamon and M. Jaime, *Rev. Mod. Phys.* **73**, 583 (2001).

³G. Catalan and J. F. Scott, *Adv. Mater.* **21**, 2463 (2009).

⁴C. A. F. Vaz, J. Hoffman, C. H. Anh, and R. Ramesh, *Adv. Mater.* **22**, 2900 (2010).

⁵Z. Cheng, X. Wang, S. Dou, H. Kimura, and K. Ozawa, *Phys. Rev. B* **77**, 092101 (2008).

⁶Z. X. Cheng, H. Y. Zhao, Y. Du, H. Kimura, K. Ozawa, and X. L. Wang, *Scripta Mater.* **65**, 249 (2011).

⁷I. Fina, L. Fabrega, X. Marti, F. Sanchez, and J. Fontcuberta, *Appl. Phys. Lett.* **97**, 232905 (2010).

⁸V. Garcia, M. Bibes, L. Bocher, S. Valencia, F. Kronast, A. Crassous, X. Moya, S. Enouz-Vedrenne, A. Gloter, D. Imhoff, C. Deranlot, N. D. Mathur, S. Fusil, K. Bouzehouane, and A. Barthelemy, *Science* **327**, 1106 (2010).

⁹T. Lottermoser, T. Lonkai, U. Amann, D. Hohlwein, J. Ihringer, and M. Fiebig, *Nature* **430**, 541 (2004).

¹⁰S. J. Luo, S. Z. Li, N. Zhang, T. Wei, X. W. Dong, K. F. Wang, and J. M. Liu, *Thin Solid Films* **519**, 240 (2010).

¹¹H. M. Jang, J. H. Park, S. W. Ryu, and S. R. Shannigrahi, *Appl. Phys. Lett.* **93**, 252904 (2008).

¹²V. B. Naik and R. Mahendiran, *J. Appl. Phys.* **106**, 123910 (2009).

¹³R. Muralidharan, T. H. Jang, C. H. Yang, Y. H. Jeong, and T. Y. Koo, *Appl. Phys. Lett.* **90**, 012506 (2007).

¹⁴B. Lorenz, Y. Q. Wang, Y. Y. Sun, and C. W. Chu, *Phys. Rev. B* **70**, 212412 (2004).

¹⁵Y. Q. Lin and X. M. Chen, *Appl. Phys. Lett.* **96**, 142902 (2010).

¹⁶P. Padhan, H. Z. Guo, P. LeClair, and A. Gupta, *Appl. Phys. Lett.* **92**, 022909 (2008).

¹⁷Y. Q. Lin, X. M. Chen, and X. Q. Liu, *Solid State Commun.* **149**, 784 (2009).

¹⁸F. Hong, Z. Cheng, H. Zhao, H. Kimura, and X. Wang, *Appl. Phys. Lett.* **99**, 092502 (2011).

¹⁹J. Hemberger, S. Lobina, H. A. K. von Nidda, N. Tristan, V. Y. Ivanov, A. A. Mukhin, A. M. Balbashov, and A. Loidl, *Phys. Rev. B* **70**, 024414 (2004).

²⁰J. Hemberger, F. Schrettle, A. Pimenov, P. Lunkenheimer, V. Y. Ivanov, A. A. Mukhin, A. M. Balbashov, and A. Loidl, *Phys. Rev. B* **75**, 035118 (2007).

²¹F. K. Chiang, M. W. Chu, F. C. Chou, H. T. Jeng, H. S. Sheu, F. R. Chen, and C. H. Chen, *Phys. Rev. B* **83**, 245105 (2011).

²²C. R. Sankar and P. A. Joy, *Phys. Rev. B* **72**, 132407 (2005).

²³R. J. Fairholme, G. P. Gill, and A. Marsh, *Mater. Res. Bull.* **6**, 1131 (1971).